land

MDPI

Article

Thermal Impacts of Synthetic Materials in Coastal Cities: A Comparative LST Analysis of Artificial Turf and Natural Grass in the Northern Adriatic

Filipa Valenčić *, Tadej Bevk and Tomaž Pipan

Department of Landscape Architecture, Biotechnical Faculty, University of Ljubljana, 1000 Ljubljana, Slovenia; tadej.bevk@bf.uni-lj.si (T.B.); tomaz.pipan@bf.uni-lj.si (T.P.)
* Correspondence: filipa.valencic@bf.uni-lj.si

Abstract

Rising summer temperatures across northern Mediterranean cities have intensified the threat of extreme heat in coastal urban areas. Urban heat island effects, driven by high density and climate change, pose a significant challenge to these coastal cities. Warming is worsened by the replacement of natural surfaces with synthetic materials for easier maintenance and lower costs—not only sports pitches but also parks, beaches and private gardens. Large artificial turf fields are of particular concern because they act as distinct heat islands, yet empirical data regarding their thermal behaviour in the northern Adriatic remain limited. While durable and water-efficient, artificial turf lacks natural cooling, leading to extreme surface temperatures and heat stress for users. In contrast, natural grass remains naturally cooler but faces high water demands, especially in dry regions. This study compared the land surface temperatures (LSTs) of artificial turf and natural grass to evaluate their thermal impact on urban microclimates. Focusing on Slovenian and Croatian Istria, seven pairs of pitches were analysed over a six-month period in 2025. NDVI trends confirmed natural grass remained predominantly green and were probably actively irrigated throughout the study. The study found that artificial turf maintained a significantly higher thermal level, with uncorrected LST showing a paired difference of 3.84 °C (peak 6.50 °C); when corrected for emissivity (cLST), the thermal gap expanded to a median paired difference of 6.28 °C (peak 9.00 °C). A linear mixed-effects model confirmed this elevation was statistically significant ($p < 0.001$; $n = 42$ paired pitch-date observations across seven pairs and six dates).

Keywords: urban heat island (UHI); land surface temperature (LST); remote sensing; artificial turf; natural grass; synthetic surfaces; Adriatic; Istria; heat mitigation; coastal regions

Check for updates

Academic Editors: Edith de Guzman, Ruth Engel, Elizabeth Wesley, Dagmar Haase and Jacques Teller

Received: 26 August 2026
Revised: 5 November 2026
Accepted: 9 November 2026
Published: 18 November 2026

Copyright: © 2026 by the authors. Licensee MDPI, Basel, Switzerland. This article is an open access article distributed under the terms and conditions of the Creative Commons Attribution (CC BY) license.

1. Introduction

1.1. Artificial Turf and Natural Grass

Artificial turf (AT), also known as synthetic turf or artificial grass, is an engineered surfacing material designed to mimic the appearance and performance of natural grass (NG). Initially introduced for use in professional indoor athletic stadiums [1], its application has since expanded to outdoor stadiums, schools and public spaces such as parks, beaches and resorts. AT is frequently favoured for its durability, longevity and perceived lower maintenance requirements, especially in dry regions where maintaining NG is difficult or

costly [2,3]. In water-scarce coastal regions, the primary advantage of AT is the elimination of the heavy irrigation required to keep NG healthy during hot, dry summers [3].

Although AT reduces localised water consumption, it entails a range of broader environmental trade-offs. Because plastic materials are largely impermeable and synthetic blades block soil contact, AT acts as an impervious surface that limits water infiltration [4]. The increased surface runoff makes AT-covered areas less suitable for locations prone to flash flooding compared to natural soil. In contrast, NG provides essential ecosystem services, such as supporting biodiversity, reducing erosion and runoff and mitigating flooding [5,6]. Furthermore, NG significantly mitigates heat through evapotranspiration and nighttime guttation—cooling processes that synthetic materials cannot perform [1,3]. Indeed, empirical studies confirm that a negative correlation between Land Surface Temperature (LST) and NDVI indicates that green areas can effectively weaken the urban heat island effect, whereas a positive correlation between LST and NDBI shows that built-up land strengthens heat accumulation in the study area [7,8].

Moreover, AT has been found to produce substantially higher surface temperatures than NG. These extreme temperatures occur because the polyethylene fibres and rubber infill of synthetic turf absorb high-intensity solar radiation—ranging from ultraviolet to near-infrared—with minimal reflectance or heat transfer to the material below [9,10]. These findings support the broader understanding that artificial materials with low albedo serve as the primary driver of temperature increases, an effect that becomes increasingly pronounced as these materials cover larger areas [11]. The efficient absorption of short-wavelength radiation causes synthetic surfaces to heat up significantly more than the surrounding ambient air [12]. Consequently, surface temperatures on AT can exceed those on NG by as much as 30 °C to 60 °C [9,13–16], surpassing asphalt and bare soil [9,13]. While NG remains close to ambient air temperatures through its cooling mechanisms, AT continues to store and radiate solar energy [3,13]. Furthermore, Mantas and Xian [17] demonstrated that AT fields across multiple sites consistently showed higher surface temperatures than nearby natural fields, with surface temperatures increasing alongside rises in ambient temperature. These findings raise concerns about the use of AT in warm climates.

While this temperature problem is manageable through irrigation, experimental results have shown that even prolonged irrigation provides only a brief cooling effect, often lasting only 5–90 min after irrigation ceases [9,13]. Cheung and Livesley [18] extended this finding by showing that while irrigation of natural vegetation provided only a minor additional cooling benefit of 1.8 °C, NG remained approximately 20 °C cooler than AT regardless of its irrigation status. This demonstrates that the fundamental thermal advantage lies in the material difference between biological and synthetic surfaces rather than in moisture levels. Although specialised heat-reduction technologies for synthetic surfaces exist, they are generally more expensive and carbon-intensive, without reaching the natural cooling efficiency of grass [6].

Consequently, users of synthetic fields—particularly children—experience more intense heat stress and a longer duration of 'extreme danger' because of higher ground temperatures and increased absorption of longwave radiation [19]. These surfaces frequently exceed the 48 °C burn threshold, reaching peaks of 71.6 °C, which can cause irreversible skin damage in just 15 s, whereas NG consistently remains below these hazardous limits [18]. This creates a profound paradox in which infrastructure designed to promote public exercise and wellness instead functions as a hazardous thermal stressor.

Beyond thermal issues, AT is a significant source of plastic pollution in aquatic environments [20] and considerable climate-altering CO_2 emissions [21]. Ultimately, while NG requires more water over its lifetime, other health and environmental considerations—such

as heat mitigation and the reduction in synthetic pollutants—often outweigh the single factor of water consumption [6].

A central insight arising from our empirical findings is the gap between regulatory land-use classifications and actual environmental performance. Municipal spatial planning documents—such as the Spatial Plan of the Municipality of Koper [22]—continue to categorise AT pitches as 'green spaces' or vegetated urban zones. This creates a paradox: synthetic surfaces lacking vegetation, evapotranspiration, and soil permeability are legally credited as contributing to municipal green targets. By treating AT as functionally equivalent to natural vegetation, spatial plans obscure localized microclimatic degradation and mask the loss of genuine ecosystem services. To bridge this planning gap, municipal zoning frameworks require immediate policy alignment. First, urban land-use codes should reclassify AT pitches as specialized synthetic sports infrastructure rather than vegetated green space, ensuring that green space ratios accurately reflect ecologically active land cover. Second, urban metrics such as the Biotope Area Factor (BAF) [23] or Green Space Factor (GSF) [24] integrated as mandatory zoning requirements in municipal spatial plans, assigning AT a performance weight of zero for thermal and ecological accounting, just as other impervious artificial surfaces. Mandating these metrics within municipal zoning codes ensures that green space targets enforce functional living vegetation rather than non-permeable synthetic substitutes.

1.2. Research Gaps

Most existing research on AT–NG temperature differences relies heavily on in situ point measurements [1,10,13,15,19]. While highly accurate, these methods lack the temporal range and wider spatial context provided by remote sensing. Even with current predictive models [12,25], there is a distinct lack of empirical observational data mapping the full spatial 'thermal footprint' of AT and NG pitches. Most data stem from short-term 'snapshots' rather than longitudinal, multi-month analyses [10,26]. To date, only a single study [17] has been identified that used remote sensing to analyse paired AT–NG pitches across multiple locations.

Furthermore, research on seasonal land surface temperature (LST) behaviour relative to air temperature is limited. Although some models address the association between LST and air temperature [3,15,27], empirical comparisons of how AT and NG interact with the surrounding air temperature over an extended season remain rare.

Finally, a significant geographical bias exists. Most data originate from either the United States [9,10,12,14,17,26] or Asia [15,19,27–30]. However, the distinct thermal regimes and Mediterranean-influenced climates of Croatian and Slovenian Istria do not necessarily reflect the climate environments represented in these existing studies. Collecting local data and establishing local patterns of AT behaviour is essential as AT becomes more common across the region. Given the climatic challenges and intensifying heat extremes of the northern Adriatic region [31], the lack of site-specific data makes it hard for planners to address the heat and ecological consequences of the increasing spread of synthetic surfaces.

1.3. Study Objectives

The primary aim of this research is to evaluate the thermal behaviour of AT and NG surfaces within the specific climatic context of the northern Adriatic region. The specific objectives are as follows:

- To compare the LSTs of AT sports pitches with those of NG sports pitches.
- To use remote sensing data and multiple measurements in a single season.
- To establish an association between ambient air temperature and the LSTs of AT and NG.

To ensure a more readable flow, the findings are presented by combining the results and discussion for each topic rather than presenting them in separate sections.

2. Materials and Methods

2.1. Site Selection and Study Area

This study focused on seven pairs of sports pitches located across seven coastal municipalities in Croatian and Slovenian Istria (Figure 1, Table 1), with each pair consisting of one AT pitch and one NG pitch. To ensure comparative consistency, candidate pitch pairs were selected based on three spatial target principles, subject to real-world infrastructure constraints across Istrian municipalities:

- Maximizing field area (>5500 m^2): Because native Landsat TIRS thermal pixels cover 10,000 m^2 (100 m × 100 m resolution), no individual sports pitch the sample (ranging from 5819.59 m^2 at Pula AT to 7986.26 m^2 at Medulin AT) is large enough to fully encompass a pure, unmixed native thermal pixel. Consequently, all satellite-derived LST values represent mixed spectral signals combining the pitch surface with adjacent land cover. Candidate selection prioritized the largest available regulation pitches (>5500 m^2) within each municipality to maximize the fractional cover of the pitch within target pixels and minimize surrounding spectral contamination.
- Coastal proximity (<1 km): To restrict the sample to the coastal maritime climate and exclude the more continentally influenced interior of Istria, all selected pitches were located within 1 km of the coastline.
- Local pair proximity (140–1350 m): Selecting pairs within a specific proximity ensured they shared the same localised microclimate, including sunlight, precipitation and air temperature, while remaining sufficiently distant from each other to prevent mutual thermal influences or sensible heat advection between field surfaces[1]. At the minimum separation distance of 142.26 m (Poreč), field centroids are separated by nearly 1.5 times the native 100 m Landsat TIRS pixel dimensions (and ~4.7 pixels in the resampled 30 m USGS grid). This spatial offset ensures that the core thermal observations remain radiometrically independent.

Table 1. Size and distance between the seven pitch pairs.

	City	Size (m^2)		Pixel Count		Distance Between Pitches (m)	AT:NG Ratio	Distance From Coast (m)	
		AT	NG	AT	NG			AT	NG
1	Koper	7820.09	7157.17	8	7	263.97	1.09	631.80	580.49
2	Umag	6805.78	7826.01	8	10	149.10	0.87	398.90	272.40
3	Novigrad	6081.31	7600.41	6	8	886.46	0.80	302.05	17.19
4	Poreč	7688.49	7777.08	11	8	142.26	0.99	538.12	644.58
5	Rovinj	7803.45	6845.97	10	9	212.31	1.14	796.20	598.52
6	Pula	5819.59	6913.74	7	8	1323.39	0.84	817.76	535.59
7	Medulin	7986.26	7604.91	8	8	337.04	1.05	127.03	334.89

The fourteen pitches were identified using OpenStreetMap geospatial data, filtered by 'pitch' and 'sport' attributes. The locations were subsequently cross-verified through high-resolution satellite imagery to confirm surface type and ensure the data reflected current land-use conditions (Figure 2).



Figure 1. Locations of the seven pitch pairs in Istria.



Figure 2. High-resolution images of each pair of pitches.

2.2. Data Acquisition and Selection Criteria

Thermal data were retrieved from the USGS (United States Geological Survey) Landsat 8 and Landsat 9 satellites (WRS-2 Path 191, Rows 028 and 029). To ensure high-quality surface observations and minimise atmospheric interference, the dataset was filtered according to the USGS Landsat Collection 2 Level-2 Science Product Guide.

The primary data-selection criterion was a maximum cloud cover threshold of 20% over the scene area. For each month between May and October 2025, a total of 3, 3, 1, 2, 1, and 1 candidate dual-tile scenes for Row 029, and 5, 6, 3, 3, 2, and 3 candidate dual-tile scenes for Row 028 met the cloud cover threshold in May, June, July, August, September, and October, respectively. To avoid selection bias toward unusually hot or clear days, scene selection was governed strictly by regular temporal spacing. From these candidate pools, only those acquisition dates were retained that simultaneously provided clear-sky coverage (<20% cloud cover) across both adjacent WRS-2 tiles (Rows 028 and 029) on the exact same day, thereby ensuring complete spatial coverage across all fourteen study pitches.

Final date selection among common candidate dates was determined by regular temporal spacing. Preference was given to the date that best preserved a consistent ~30–40 day sampling interval relative to adjacent dates, independent of daily surface or ambient temperatures[2].

To evaluate potential localized atmospheric and retrieval noise, per-pixel screening was performed using the Landsat Collection 2 QA_PIXEL mask (evaluating cloud, cloud shadow, cirrus, and dilated cloud flags). Out of 84 total pitch-date observations, 83 were confirmed to be completely clear of cloud and shadow interference, with only a single observation (Medulin AT on 10 June 2025) triggering a cloud/shadow flag. Additionally, per-pixel Surface Temperature Retrieval Uncertainty (ST_QA) values were extracted (available as Supplementary Material), ranging between 1.85 K and 6.04 K across the dataset (1.85–5.15 K in October). Because systematic atmospheric retrieval errors affect adjacent targets identically within the same scene, these absolute uncertainties cancel out in relative pairwise differences ($\Delta LST = LST_{AT} - LST_{NG}$), leaving spatial microclimate contrasts robust.

Landsat TIRS data were collected natively at 100 m resolution and resampled to 30 m by the USGS. Satellite overpasses occurred at ~11:50 a.m. CEST (09:52 UTC), capturing surfaces under high solar illumination roughly 1.2 h prior to local solar noon (~13:05 CEST) and thereby minimising shadowing.

Hourly air temperature data were sourced from official meteorological stations operated by ARSO (Slovenia) and DHMZ (Croatia), with measurements synchronised to the specific satellite overpass times to ensure data consistency. Consequently, the study was restricted to Koper, Pula and Poreč; other regional sites were excluded because of a lack of standardised monitoring infrastructure required for scientific validation. Detailed station metadata, including network identifiers, spatial coordinates, elevations, estimated WMO/CIMO siting classes, and distances to target pitches, are summarized in Table 2.

To evaluate background environmental influence arising from pixel mixing, land cover within a 100 m buffer around each pitch boundary was classified into percentage of impervious cover using data from the Copernicus Land Monitoring Service (CLMS) CORINE Land Cover (CLC) backbone. Ordinary Least Squares (OLS) regression models were fitted to test the interaction effect (LST ~ Surface × Impervious_Pct) and an additive ANCOVA model (LST ~ Surface + Impervious_Pct) to isolate the direct surface material effect from surrounding urban microenvironments.

Table 2. Metadata for ground-based meteorological stations used in the analysis.

Station	Network	ID	Coordinates	Elevation (m a.s.l.)	Estimated Siting Class[3]	Distance to Pitch (km)	
						AT	NG
Koper — Kapitanija	ARSO	2293	Y: 400,413 m, X: 46,147 m (D96/TM) (45.5481° N, 13.7245° E)	4	4	1.77	1.57
Pula	DHMZ	14307	44.894° N, 13.922° E	63	2–3	6.69	7.99
Poreč	DHMZ	14301	45.2333° N, 13.600° E	15	3	4.27	4.25

2.3. Land Surface Temperature Modelling

LST modelling was performed using ArcGIS Pro 3.4.0. The original, uncorrected Landsat Level-2 Surface Temperature (ST) product was used for all primary thermal analyses and statistical comparisons across pitches. The initial Landsat LST products used emissivity values derived from the ASTER Global Emissivity Database (GED), which are dynamically adjusted for vegetation fraction using scene NDVI according to the Collection 2 algorithm [32].

While the ASTER GED is a standard for emissivity, its coarse resolution (100 m) and reliance on a 2000–2008 climatology [33] may not reflect recent land-cover changes, such as the installation of synthetic turf pitches in the study area, nor does it account for the specific spectral signatures of polymers and rubber infill. Because AT can reach extreme temperatures, accurate emissivity estimates are extremely important; a minor discrepancy can result in a significant error in the final LST calculation.

To test the sensitivity of the retrieval and evaluate potential radiometric bias for small-scale synthetic surfaces, a secondary emissivity correction was performed. AT emissivity was corrected to 0.95, a value consistent with synthetic polymers and crumb rubber reported in urban thermal studies [7,15,34], while the emissivity of NG was corrected to 0.98 [33,35].

Per-pixel product emissivity (ST_EMIS) was extracted for each pitch, and the radiometric test was applied using the atmospheric bands provided in the Level-2 product (ST_TRAD, ST_URAD, ST_DRAD, and ST_ATRAN) [36]. Radiance under target emissivity values was calculated via single-channel radiative transfer [37]:

$$B(T_s) = \frac{ST_TRAD - ST_URAD - (1-\varepsilon_{target}) \times ST_DRAD}{\varepsilon_{target} \times ST_ATRAN} \quad (1)$$

where $B(T_s)$ is the Planck thermal radiance at surface temperature T_s; ε_{target} is the target emissivity (0.95 for AT; 0.98 for NG); and ST_TRAD, ST_URAD, ST_DRAD, and ST_ATRAN represent thermal radiance, upwelling radiance, downwelling radiance, and atmospheric transmittance, respectively [36]. The adjusted surface temperature (T_s, in Kelvin) was obtained by inverting $B(T_s)$ using the Landsat Band 10 thermal constants (K_1 and K_2) [36].

Following the original LST data extraction, zonal statistics were used to calculate the mean, minimum, maximum, median, 25th and 75th percentiles and standard deviation of LST data for each pitch. Using the pitch boundary polygons as zones, the LST value of each pixel within each zone was extracted to characterise the thermal environment of each pitch. Together, these statistics formed the dataset used for seasonal comparisons across all chosen dates. This analysis was conducted across all pitches for each observation date.

To assess differences in LST between AT and NG, paired temperature differences were calculated for each location and date (ATmedian–NGmedian), resulting in 42 paired observations across seven location and six dates. As repeated observations share spatial context and temporal conditions on the date of measurements, a linear mixed-effects model was chosen to test for differences. The model was fitted to the paired differences, with an

intercept as the sole fixed effect and using location and date as crossed random intercepts. This approach accounted for the non-independence of repeated observations from the same locations and measurements collected on the same dates and allows the magnitude of LST difference to vary systematically across spatial and temporal contexts. The fixed intercept represents the estimated mean difference between the median LST values of the two surface types. The random-effect variance components quantified variation in this difference among locations and dates.

The models were created in R 4.6.1 with lme4 and lmerTest packages, using Restricted Maximum Likelihood (REML) as estimation method. The statistical significance of the fixed intercept was assessed using t-test with Satterthwaite-approximated degrees of freedom. Fixed effect estimates are reported with 95% confidence intervals. The supplementary data (Supplementary Figure S1) include model diagnostics (residual distribution and fitted-versus-residual plots).

3. Results and Discussion

3.1. Baseline Product Emissivity

Per-pixel baseline product emissivity values (ST_EMIS) extracted from the Landsat Level-2 product across all seven pitch pairs and six observation dates are presented in Table 3. Native algorithm emissivity values for artificial turf (AT) ranged between 0.964 (Koper, across all observation dates) and 0.981 (Poreč, 1 May). For natural grass (NG), native emissivity ranged between 0.965 (Novigrad, 10 June and 13 August) and 0.987 (Poreč, 1 May and 10 June).

Table 3. Landsat Level-2 baseline product emissivity values for artificial turf (AT) and natural grass (NG) across six acquisition dates in 2025.

2025		1 May	10 June	20 July	13 August	6 September	8 October
Koper	AT	0.965	0.965	0.965	0.965	0.965	0.965
	NG	0.970	0.969	0.970	0.969	0.970	0.970
Umag	AT	0.976	0.975	0.976	0.975	0.976	0.976
	NG	0.983	0.982	0.983	0.982	0.983	0.983
Novigrad	AT	0.969	0.968	0.969	0.968	0.969	0.969
	NG	0.956	0.954	0.956	0.954	0.956	0.956
Poreč	AT	0.981	0.980	0.980	0.980	0.981	0.981
	NG	0.987	0.987	0.985	0.985	0.985	0.986
Rovinj	AT	0.980	0.980	0.980	0.979	0.980	0.980
	NG	0.970	0.969	0.970	0.969	0.970	0.970
Pula	AT	0.975	0.974	0.975	0.974	0.975	0.975
	NG	0.971	0.970	0.971	0.970	0.971	0.971
Medulin	AT	0.969	0.968	0.969	0.968	0.969	0.969
	NG	0.9741	0.9729	0.9741	0.9729	0.9741	0.9741

Across most target locations, native ST_EMIS values for AT were relatively high (averaging ≈ 0.972), reflecting the Collection 2 dynamic vegetation-cover algorithm, which adjusts baseline ASTER GED values using scene NDVI. Because synthetic pitches occupy small surface areas relative to the 30 m thermal pixel grid, pixel mixing with surrounding vegetated borders elevates the effective NDVI, causing the automated retrieval to assign soil- or vegetation-weighted emissivity rather than pure polymer values. In specific instances (e.g., Novigrad, Pula and Rovinj), native ST_EMIS values for AT slightly exceeded those of adjacent NG pitches.

To quantify the thermal impact of this algorithm behavior, a single-channel radiometric sensitivity test was conducted using Level-2 atmospheric parameters (ST_TRAD,

ST_URAD, ST_DRAD, and ST_ATRAN) under fixed target emissivities ($\varepsilon_{AT} = 0.95$ and $\varepsilon_{NG} = 0.98$). Table 4 summarizes the mean uncorrected (LST) and corrected (cLST) land surface temperatures and surface temperature differences ($\Delta LST_{AT–NG}$) across all sites and dates.

Table 4. Comparison of median uncorrected ($LST_{AT–NG}$) and corrected ($cLST_{AT–NG}$) surface temperature differences (°C) and the resulting adjustment offset ($\Delta LST_{AT–NG}$) across sites and dates.

		Koper	Umag	Novigrad	Poreč	Rovinj	Pula	Medulin
1 May	$cLST_{AT-NG}$	6.97	5.70	9.00	7.00	8.92	4.61	6.23
	LST_{AT-NG}	5.15	3.64	6.50	5.49	6.22	1.91	4.89
	Δ cLST-LST	1.81	2.06	2.49	1.51	2.69	2.70	1.34
10 June	$cLST_{AT-NG}$	8.23	6.64	6.23	6.89	6.38	4.83	6.19
	LST_{AT-NG}	6.39	4.55	3.78	5.25	3.70	2.06	4.50
	Δ cLST-LST	1.84	2.09	2.45	1.64	2.68	2.76	1.69
20 July	$cLST_{AT-NG}$	6.41	6.71	7.34	7.82	6.70	6.32	7.19
	LST_{AT-NG}	4.60	4.73	4.61	6.16	4.27	3.60	5.82
	Δ cLST-LST	1.81	1.99	2.73	1.67	2.43	2.72	1.37
13 August	$cLST_{AT-NG}$	7.66	6.44	8.47	7.72	6.53	4.79	5.22
	LST_{AT-NG}	5.74	4.26	5.51	6.21	3.97	2.06	3.57
	Δ cLST-LST	1.92	2.17	2.96	1.51	2.56	2.74	1.65
6 September	$cLST_{AT-NG}$	4.38	3.51	4.93	6.53	5.44	3.25	4.95
	LST_{AT-NG}	2.66	1.62	2.11	4.85	2.75	0.73	3.41
	Δ cLST-LST	1.73	1.89	2.83	1.68	2.68	2.52	1.54
8 October	$cLST_{AT-NG}$	4.70	4.16	3.96	4.43	4.78	1.96	3.50
	LST_{AT-NG}	3.02	2.39	1.46	2.95	2.50	−0.31	1.87
	Δ cLST-LST	1.67	1.78	2.51	1.48	2.29	2.27	1.63

Adjusting emissivity systematically inflated the retrieved thermal gap between AT and NG across all 42 paired comparisons, introducing an additional thermal offset Δ cLST-LST ranging between 1.34 °C (Medulin, October) and 2.96 °C (Novigrad, August). Across all locations and dates, the secondary adjustment added an average of ≈2.05 °C to the observed AT–NG temperature difference. The impact was particularly notable in scenes with slight baseline emissivity inversions; for example, in Pula on 10-08, where native algorithm assumptions yielded an uncorrected median difference of −0.36 °C (NG warmer than AT), the single-channel adjustment shifted the difference to +2.02 °C.

Because native emissivity values for AT remain higher than pure polymer and crumb rubber spectra ≈ 0.95, the uncorrected product provides a conservative lower-bound estimate of synthetic surface overheating. Conversely, forcing target emissivities of 0.95 and 0.98 establishes a theoretical upper-bound thermal difference. Importantly, while the secondary correction modulates the absolute magnitude of the thermal gap (accounting for roughly 20% to 42% of the adjusted values depending on site and date), the primary scientific conclusion remains robust under both models: artificial turf exhibits statistically significant and severe surface overheating relative to natural grass across all observed months. Native product LST values are therefore retained for primary statistical and spatiotemporal comparisons in subsequent sections to avoid introducing artificial post-processing bias.

To evaluate retrieval response across reported synthetic material spectra, a sensitivity analysis was conducted across $\boldsymbol{\varepsilon_{AT}} = 0.90–0.97$ for the peak summer scene (20 July 2025) (Table 5). Decreasing $\boldsymbol{\varepsilon_{AT}}$ from 0.97 to 0.90 systematically elevated median surface temperatures by an average of ≈5.0 °C. Even at $\boldsymbol{\varepsilon_{AT}} = 0.97$, median AT temperatures reached up to 47.42 °C (Pula), confirming that synthetic turf warming remains significant across all realistic emissivity parameterizations.

Table 5. Sensitivity of median artificial turf (AT) land surface temperature (LST, °C) across a range of target emissivity values (εAT = 0.90–0.97) on 20 July 2025.

City/ ε_{AT}	0.90	0.93	0.95	0.97
Koper	51.22	48.98	47.54	46.15
Umag	52.13	49.87	48.42	47.01
Novigrad	48.60	46.40	44.99	43.62
Poreč	43.78	41.65	40.30	38.98
Rovinj	52.28	50.01	48.56	47.15
Pula	52.59	50.30	48.84	47.42
Medulin	49.05	46.83	45.40	44.02

3.2. Thermal Maps

The visual comparison of the spatial distribution of isotherms revealed a clear difference between the surface types across all locations (Figure 3). While bicubic resampling was applied to the 30 m resolution data solely to smooth thermal contours for visual presentation, the underlying pixel-level Land Surface Temperature (LST) values demonstrate consistent thermal divergence between artificial turf (AT) and natural grass (NG).

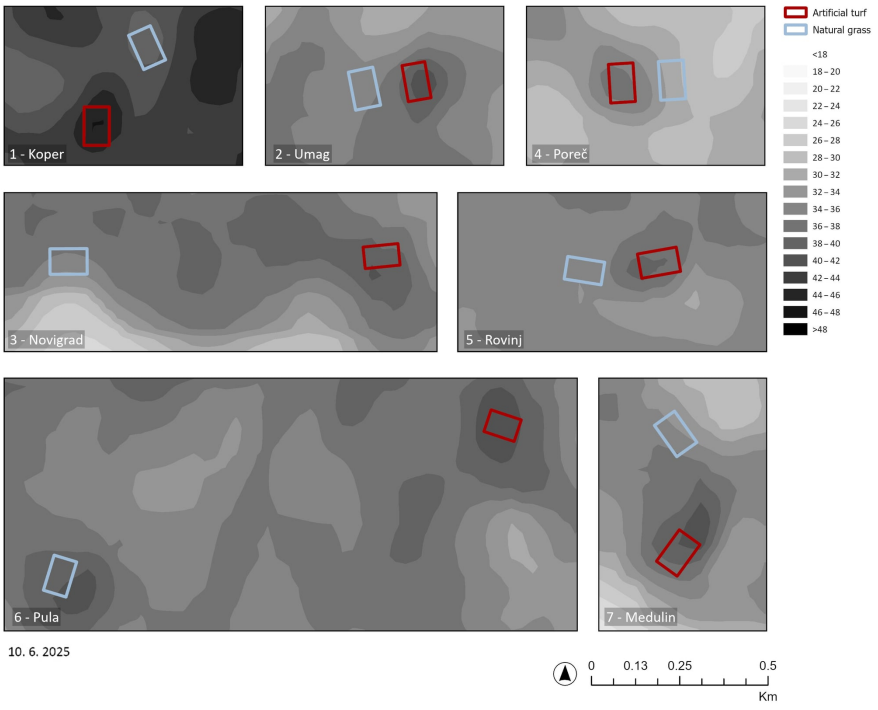


Figure 3. Thermal maps of land surface temperatures at the seven locations on 10 June 2025 . Red outlines indicate artificial turf pitches and blue outlines indicate natural grass pitches. The thermal maps were bicubically resampled from their 30 m resolution to create smoother transitions between temperature zones.

The thermal maps showed that AT pitches acted as 'hot spots' within their immediate urban surroundings, consistently reaching temperatures in the upper ranges of the scale, even when compared to built areas. NG pitches, however, appeared thermally neutral, with their LSTs being subject to their surroundings. When influenced by local factors such as sea breezes and coastal air, they maintained lower temperatures, such as the NG pitch in Novigrad, aligning with findings that coastal area LSTs are affected by sea–breeze circulation [38].

In contrast, AT showed elevated surface temperatures across all study sites regardless of how close they were to the coast. Rather than actively overriding coastal cooling, this behavior simply reflects how synthetic materials handle heat. Unlike natural grass, artificial turf cannot cool itself through evaporation because it contains no moisture. Without this natural evaporative cooling, synthetic pitch surfaces absorb solar energy and reach much higher baseline temperatures, regardless of surrounding breezes.

This heat behavior (Table 6) was clear at coastal sites such as Medulin, where AT maintained high temperatures (36–38 °C) despite being right next to the sea. While ambient sea breezes provide advective cooling, the absence of evaporative heat loss prevents synthetic turf from reaching lower equilibrium temperatures. As a result, building synthetic pitches in coastal areas does not automatically prevent surface overheating, as the lack of moisture prevents these surfaces from taking advantage of cooler coastal air to reduce surface temperatures to levels comparable with natural grass.

Table 6. Date-averaged within-pitch statistics. Min = Minimum; Max = Maximum; SD = Standard Deviation; Pct = Percentile.

Location	Surface	Count	Min	Max	Range	Mean	SD	Median	Pct25	Pct75	Pct90
Koper	AT	8	40.33	41.46	1.14	40.98	0.39	41.06	40.73	41.28	41.41
Koper	NG	7	36.18	37.28	1.10	36.62	0.39	36.47	36.32	36.87	37.14
Umag	AT	8	36.06	38.52	2.46	37.29	0.87	37.29	36.65	38.04	38.30
Umag	NG	10	33.11	34.78	1.66	33.84	0.50	33.76	33.47	34.11	34.49
Novigrad	AT	6	37.11	38.92	1.82	37.95	0.65	37.93	37.43	38.37	38.71
Novigrad	NG	8	33.06	34.54	1.47	33.81	0.54	33.93	33.28	34.24	34.38
Poreč	AT	11	33.06	35.77	2.71	34.65	0.82	34.76	34.14	35.30	35.53
Poreč	NG	8	28.96	30.41	1.46	29.67	0.52	29.61	29.24	30.12	30.30
Rovinj	AT	10	36.38	38.46	2.08	37.50	0.62	37.49	37.15	37.90	38.23
Rovinj	NG	9	33.34	34.10	0.76	33.63	0.25	33.59	33.44	33.73	33.94
Pula	AT	7	38.49	40.16	1.67	39.41	0.58	39.46	39.02	39.87	40.04
Pula	NG	8	36.87	38.21	1.33	37.68	0.40	37.79	37.50	37.93	38.06
Medulin	AT	8	35.28	38.40	3.12	36.81	1.07	36.86	35.97	37.66	38.08
Medulin	NG	8	32.25	33.47	1.21	32.83	0.41	32.85	32.50	33.14	33.30

3.3. AT–NG: Spatiotemporal Analysis of LST Variations

Across all seven locations, the results showed a consistent pattern despite minor local differences. Time-series analysis (Figure 4) revealed that LSTs for both AT and NG followed the same seasonal cycle, peaking in mid-summer (July–August). In the original LST dataset, the gap was not constant: it increased as the sun became stronger, reaching maximum differences of 2.06–6.69 °C in June, with AT median temperatures reaching peak extremes above 50 °C in Koper. As illustrated in Figure 4, while the magnitude of the gap varied slightly by city—with Poreč exhibiting a consistently elevated gap throughout mid-summer—a thermal penalty persisted across most sites year-round. In the original LST baseline, during the October cooling phase, differences ranged from −0.31–3.02 °C across locations, with Pula recording the lowest seasonal difference, briefly dropping slightly below zero (−0.31 °C).

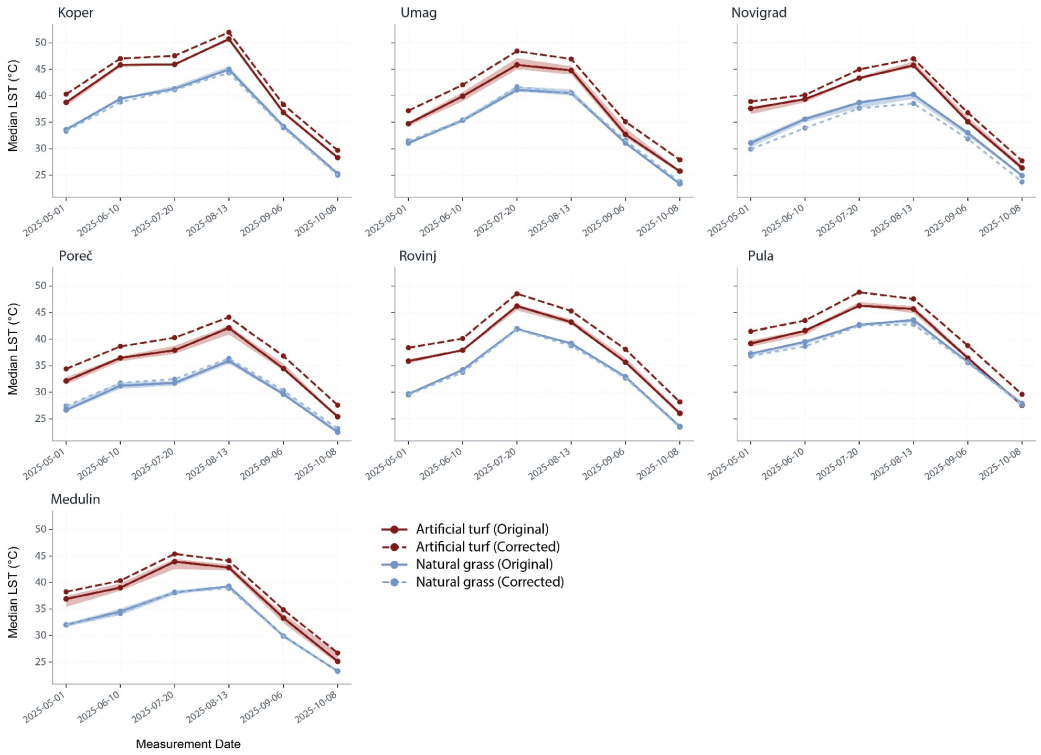


Figure 4. Comparative median land surface temperature trajectories for artificial turf and natural grass for each of the seven locations over six dates (solid lines represent original LST values; dashed lines represent corrected LST values).

Comparing these original LST trajectories with the emissivity-corrected LST values (represented by the dashed lines in Figure 5) demonstrates that adjusting for surface emissivity systematically elevates the thermal profile of AT across all sites while NG baselines remain almost unchanged. Consequently, emissivity correction expands the thermal difference between synthetic and natural surfaces across the entire observation period. In the corrected dataset, the overall mean paired AT–NG median LST difference reached 6.28 °C (Table 4), spanning a seasonal range from 1.96 °C (Pula) to 9.00 °C (Novigrad). This pronounced thermal margin in Novigrad coincides with notable within-pair spatial asymmetries, as its artificial turf pitch is situated 302 m from the shoreline while the natural grass counterpart lies just 17 m away. While this coastal proximity may provide additional microclimatic cooling to the natural grass site, it likely operates alongside the fundamental material differences established in Section 3.2, where the lack of evaporative heat loss on synthetic surfaces limits their capacity to benefit from localized marine cooling. Corrected peak differences exceeded the original mid-summer range, reaching a mean of 6.63 °C on 20 July (peaking at 7.82 °C in Poreč) and 6.69 °C on 13 August (peaking at 8.47 °C in Novigrad). Furthermore, during the October cooling phase, corrected differences remained distinctly higher than original estimates, averaging 3.93 °C across sites, with Pula maintaining a positive difference of 1.96 °C rather than dropping below zero (−0.31 °C). Across individual municipalities, Poreč (6.95 °C gap), Novigrad (6.78 °C), Koper (6.69 °C), and Rovinj (6.45 °C) exhibited the highest overall corrected median thermal gaps.

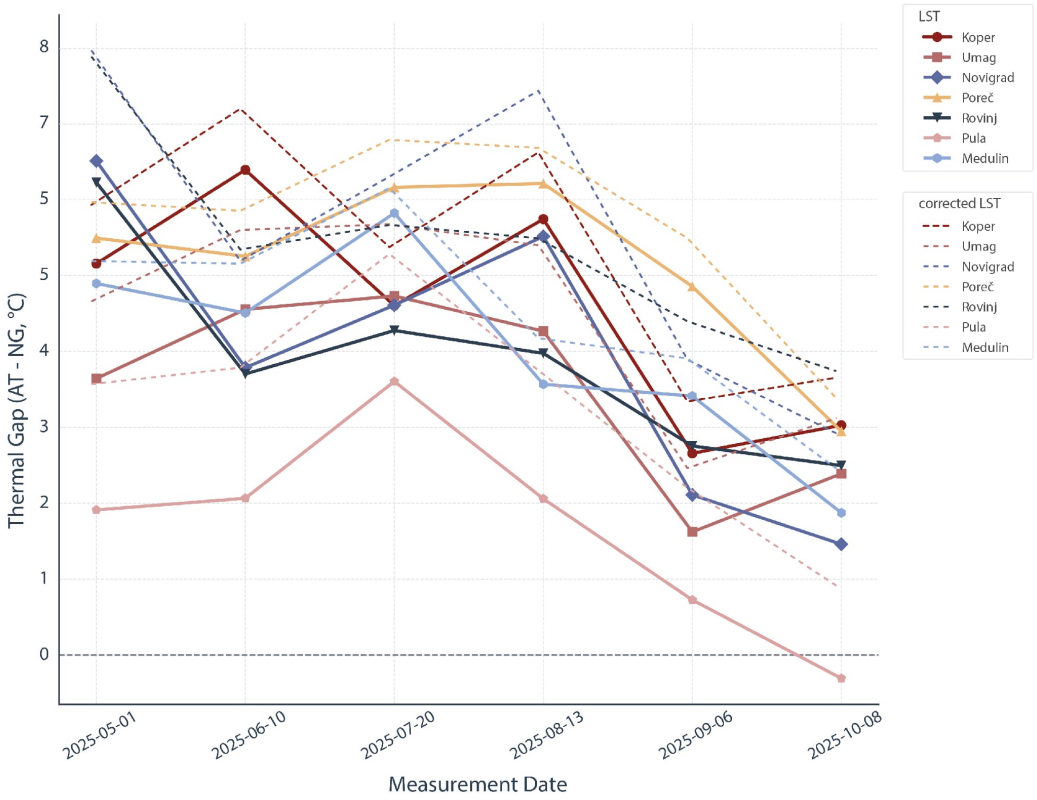


Figure 5. Comparison of paired land surface temperature (LST) differences ($\Delta LST = LST_{AT} - LST_{NG}$) across seven locations over six measurement dates in 2025. Solid lines with markers represent the original extracted LST differences; dashed lines without solid markers represent the emissivity-corrected LST differences.

Detailed boxplot profiles across multiple dates (1 May–8 October) of the non-corrected LST confirm distinct thermal regimes between artificial turf (AT) and natural grass (NG) pitches across all studied locations (Figure 6). When compared within the same city, thermal distributions between the two surface types exhibited minimal to no overlap on individual observation dates. On nearly every recorded date, the interquartile range of AT was higher than that of NG at the corresponding location. This thermal divergence peaked during mid-summer (20 July and 13 August), when the minimum temperatures recorded on AT routinely exceeded the maximum temperatures recorded on NG within the same municipality.

The width of the boxplots further reveals notable differences in spatial temperature dispersion across the delineated pitch zones. While NG boxplots generally remained compact—reflecting a consistently narrow interquartile range across most dates—AT boxplots exhibited a wider and more variable distribution overall. However, this broader spread cannot be interpreted as internal sub-pitch thermal variance or localized material hotspots. Given the native thermal resolution of the Landsat 8 and 9 sensors (resampled to 30 m), individual pitches are represented by very few native thermal pixels. Consequently, this within-pitch dispersion is dominated by spatial edge-mixing effects along pitch boundaries, where the intense thermal emission of synthetic turf blends with cooler surrounding land covers, rather than internal surface heterogeneity.

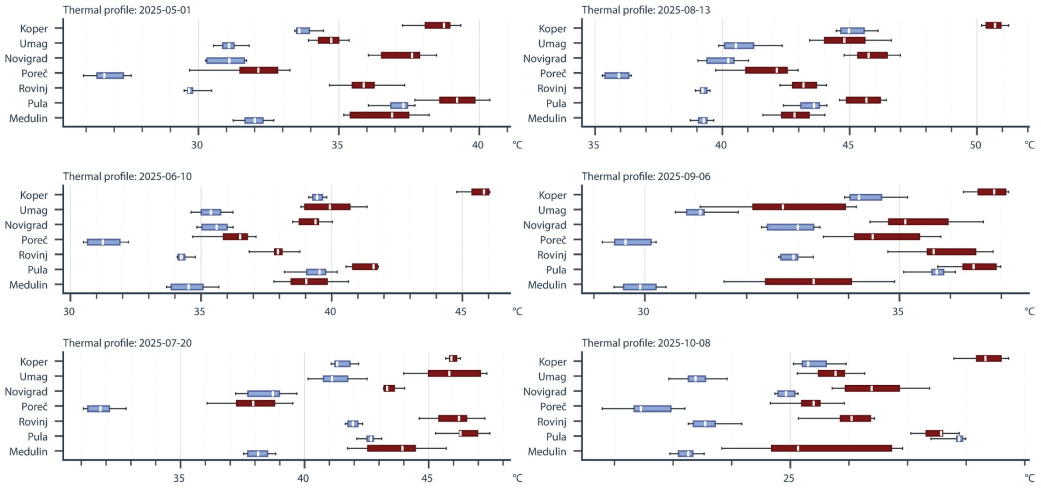


Figure 6. Thermal profile boxplots displaying the median, quartiles and range for artificial turf and natural grass across each city and measurement date.

3.4. Comparative Analysis

3.4.1. Mixed-Effects Analysis of Paired Temperature Differences

The linear mixed model revealed a statistically significant difference in median land surface temperature on AT and NG pitches after accounting for repeated measurements across seven locations and six observation dates (Table 7). On average, AT pitches exhibited temperatures 3.84 °C higher compared to NG pitches (SE = 0.64 °C, 95% CI = 2.40 − 5.27 °C, $t(9.422) = 6.011$, $p < 0.001$).

Table 7. Linear mixed-effects model of paired AT-NG LST differences (n = 42).

Fixed Effect	**Estimate [°C]**	**Std. Error [°C]**	**95% CI [°C]**	**Significance**
Mean AT-NG difference [°C]	3.837	0.638	2.403–5.271	$t = 6.011$ $p < 0.001$
Random Effects	**Variance [°C^2]**	**Std. Dev. [°C]**	**Share of Total Variance**	
Location (intercept)	1.080	1.039	34.3%	
Date (intercept)	1.428	1.195	45.4%	
Residual	0.641	0.800	20.4%	

The random-effects estimates indicate that the magnitude of the temperature difference varies across both locations and measurement dates. The estimated between-location variance was 1.080 °C^2 (SD = 1.039 °C) and the between-date variance was 1.428 °C^2 (SD = 1.1950 °C). The residual variance was 0.6409 °C^2 (SD = 0.8005 °C). Based on the estimated variance components, approximately 45.4% of modelled variance in the AT-NG temperature difference is associated with systemic differences between dates, 34.3% is associated with differences between sites and 20.4% is residual. The greater estimated between-date variance suggests that temporal heterogeneity in the temperature differences was more pronounced than spatial heterogeneity within the study sample, potentially suggesting an effect of seasonality on temperature differences. Overall, these results demonstrate that AT pitches have significantly higher LST compared to NG pitches during the study period, although the magnitude of this difference changes between locations and dates.

3.4.2. Impact of Surrounding Land Cover

To address background thermal contamination resulting from Landsat's native 100 m TIRS pixel resolution, land cover within a 100 m buffer surrounding each pitch was classified into percentage of impervious cover (*Impervious_Pct*). Two Ordinary Least Squares (OLS) regression models were evaluated to test background environmental influence against direct surface material effects.

First, an interaction model (LST ~ Surface × Impervious_Pct) evaluated whether the thermal gap between artificial turf (AT) and natural grass (NG) varied systematically with surrounding built density. The interaction term was not statistically significant ($\beta = 0.0380$, $p = 0.280$, 95% CI [−0.04, 0.11] °C per percentage point of impervious cover). Although this provides no evidence of a systematic interaction effect, the width of the confidence interval across the 0–80% cover range does not preclude a modest differential response, indicating that background independence should be stated with appropriate caution (Figure 7).

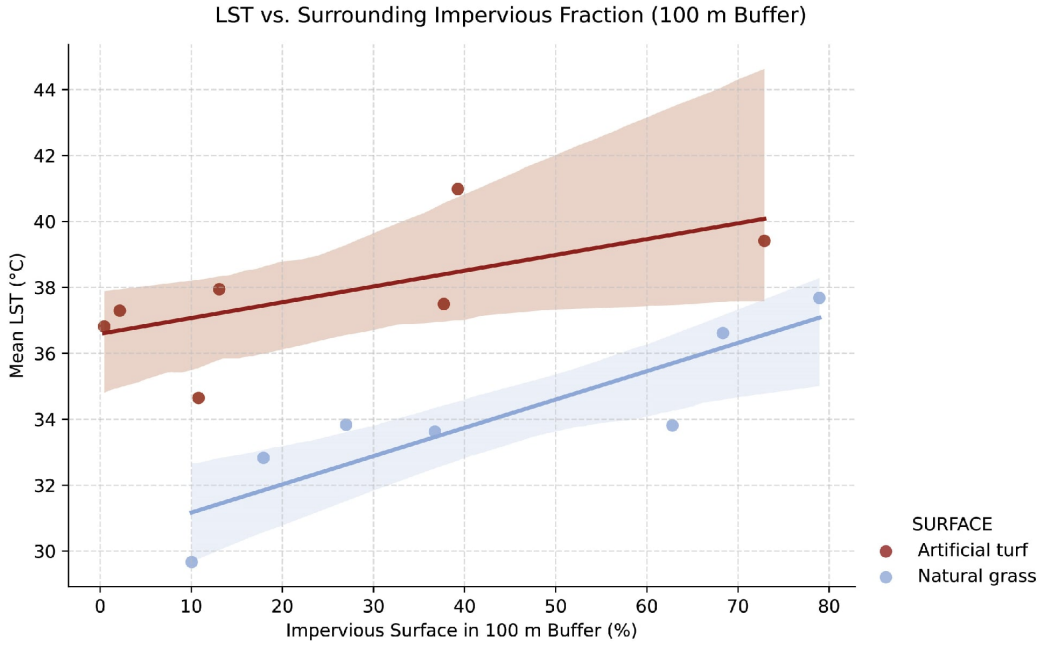


Figure 7. Relationship between mean Land Surface Temperature (LST) and impervious surface percentage within a 100 m buffer across Artificial Turf (red) and Natural Grass (blue) pitches. Shaded areas represent 95% confidence intervals. Both surface types show a positive baseline warming trend with increasing background built cover (Model 2: $\beta = 0.0673$, $p = 0.002$). The parallel slope trajectories confirm the absence of a statistically significant interaction effect (Model 1: $p = 0.280$), while the consistent vertical separation illustrates the adjusted 4.99 °C thermal gap referable to surface material differences.

Second, an additive ANCOVA model (LST ~ Surface + Impervious_Pct) was fitted to isolate the direct surface material effect while controlling for microenvironmental background warmth. Surrounding buffer imperviousness significantly predicted pitch-level LST ($\beta = 0.0673$, $p = 0.002$, $R^2_{adj} = 0.728$), contributing approximately 0.67 °C of additional surface warmth for every 10% increase in surrounding impervious cover. After controlling for background imperviousness, the isolated effect of surface material remained highly significant ($F(2, 11) = 18.43$, $p < 0.001$). Under covariate control, Natural Grass maintained an adjusted mean surface temperature 4.99 °C lower than Artificial Turf (95% CI [−6.94 °C, −3.05 °C]). Crucially, the covariate-adjusted difference (4.99 °C) exceeds the raw unadjusted mean difference (3.79 °C) surrounding built cover served to mask rather than inflate the

material-driven contrast, rendering the raw unadjusted gap a conservative lower bound of the true thermal impact.

3.5. Relationship Between Air Temperature and LST

Linear regression of LST against ambient air temperature demonstrated that while surface temperatures tracked regional atmospheric conditions, AT consistently maintained higher absolute thermal profiles than NG across all dates (Figure 8, Table 8). In individual site models, R^2 values indicated that air temperature was a strong predictor of LST in Poreč ($R^2 = 0.98$ for AT; $R^2 = 0.97$ for NG), whereas greater statistical dispersion was observed in Koper ($R^2 = 0.62$ for AT; $R^2 = 0.71$ for NG), likely reflecting localized coastal microclimatic influences such as sea breezes.

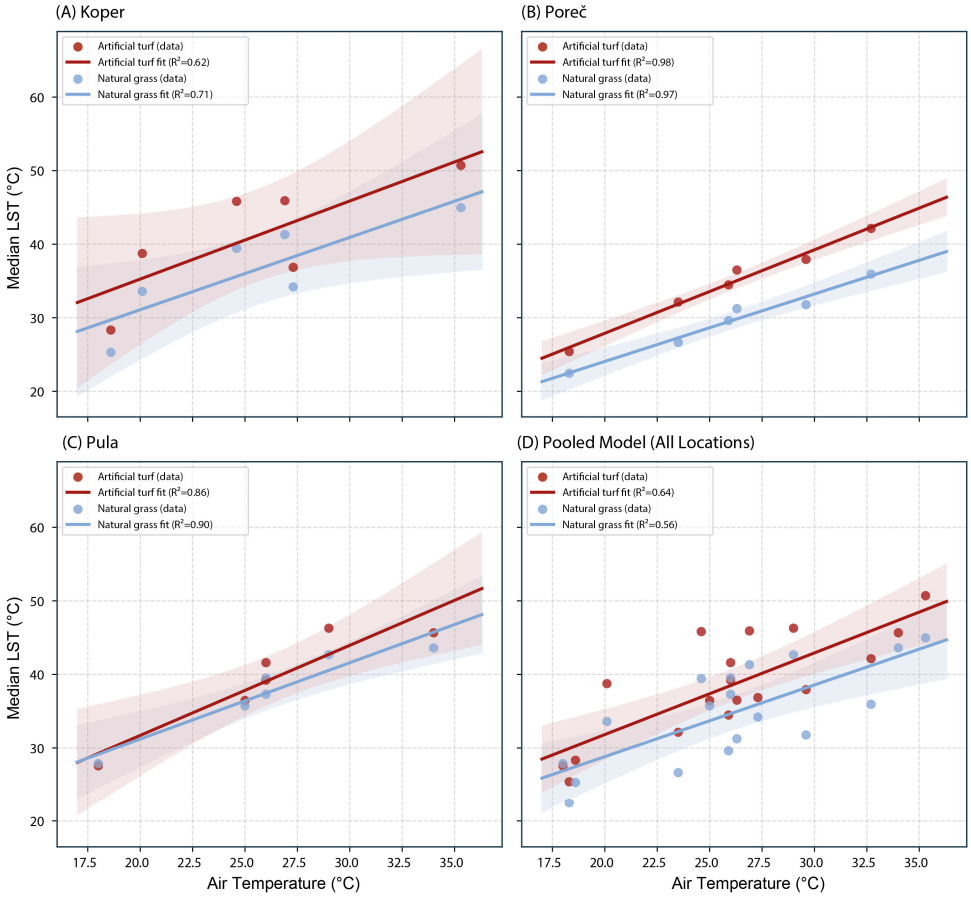


Figure 8. Linear regression analysis of median land surface temperature (°C) against air temperature (°C) for artificial turf (red) and natural grass (blue). Solid lines represent the fitted regressions, and the shaded bands represent the 95% confidence intervals of the predicted mean fit. Pooled model (N = 36) testing confirmed that slopes for both surfaces do not significantly exceed 1.0, and the slope interaction between surface types is non-significant ($\Delta\beta = 0.140$, $p_2 = 0.6437$).

To evaluate whether AT exhibits a steeper thermal sensitivity (i.e., slope $\beta > 1.0$) compared to NG across the sampling campaign, a pooled linear interaction model was applied (N = 36, overall full interaction model, $R^2 = 0.60$; individual group fits: $R^2 = 0.64$ for AT, $R^2 = 0.56$ for NG). The pooled slope for AT was estimated at $\beta = 1.110$ (95% CI: 0.670–1.550), while the pooled slope for NG was $\beta = 0.970$ (95% CI: 0.520–1430, SE = 0.214, $p_2 = 0.0003$). However, a one-tailed test comparing this slope against unity (H_0: $\beta = 1.0$) showed no statistically significant elevation above 1.0 ($t = 0.52$, $p_1 = 0.6066$). Furthermore, the interaction between air temperature and surface type was not statistically significant ($\Delta\beta = 0.140$,

$p_2 = 0.6437$), indicating that the empirical scaling of LST relative to air temperature does not differ significantly between AT and NG in this coastal setting.

Table 8. Regression coefficients and 95% confidence intervals for land surface temperature (LST) versus air temperature across individual study sites and the pooled interaction model ($N = 36$).

Site/Model	Surface	Slope (β)	Standard Error (SE)	95% Confidence Interval	R^2	p_1-Value (H_0: β = 1)	p_2-Value (H_0: β = 0)
Koper	AT	1.06	0.414	[−0.09, 2.21]	0.62	0.8886	0.0625
	NG	0.98	0.312	[0.12, 1.85]	0.71	0.9613	0.0344
Poreč	AT	1.13	0.081	[0.91, 1.36]	0.98	0.1747	0.0002
	NG	0.92	0.086	[0.68, 1.15]	0.97	0.3855	0.0004
Pula	AT	1.22	0.249	[0.53, 1.92]	0.86	0.4181	0.0079
	NG	1.04	0.168	[0.57, 1.50]	0.90	0.8330	0.0035
Pooled Model	AT	1.11	0.210	[0.67, 1.55]	0.64	0.6066	<0.0001
	NG	0.97	0.214	[0.52, 1.43]	0.56	0.9056	0.0003
	Interaction (Δβ)	0.14	0.300	[−0.47, 0.75]	0.60	-	0.6437

These observed slopes ($\beta = 1.110$) are substantially more moderate than response ratios reported in continental studies, where surface temperature increases of 2.5:1 to 5:1 per 1 °C of air warming have been documented during summer peaks [9,12]. While these findings describe a clear empirical relationship, the present analysis evaluates air temperature as a co-varying descriptive proxy rather than an isolated causal mechanism. Because air temperature and solar irradiance are collinear across the six sampling dates (spanning May to October), a 25 °C observation in spring reflects a distinct solar elevation and insolation profile compared to a 25 °C observation in autumn. As highlighted by Jim [15] and Vyrlas [13], direct solar radiation exerts a fundamental influence on surface heating, often elevating LST above 70 °C even under moderate ambient air temperatures. Consequently, the observed thermal baselines represent the combined influence of atmospheric conditions and seasonal solar forcing, with the regional Adriatic maritime climate acting to moderate peak surface thermal extremes.

3.6. Methodological Considerations and Study Limitations

A primary concern is the native resolution. Because native thermal pixels cover 10,000 m^2 (100 m × 100 m resolution), no individual sports pitch in the sample (ranging from 5819.59 m^2 to 7986.26 m^2) fully encompasses an unmixed pixel. Consequently, all satellite-derived LST values represent mixed spectral signals combining the pitch surface with adjacent land cover. While establishing a >5500 m^2 size threshold maximized fractional pitch cover within target pixels, the resulting LST values still represent an integrated thermal response. Our buffer analysis demonstrates that surrounding built environments impart a baseline warming effect on both surface types ($\beta = 0.0673$, $p = 0.002$). As a result, the raw unadjusted mean temperature difference of 3.79 °C represents a conservative lower-bound estimate, as surrounding microenvironmental warmth partially masks the material differential. When controlling for surrounding background land cover via ANCOVA ($p < 0.001$), the isolated surface material effect of AT over NG widens to an adjusted mean difference of 4.99 °C.

Another concern is the use of a fixed emissivity (0.95) for AT. While this adjustment is a significant improvement over outdated ASTER GED products and aligns with synthetic polymer standards, it assumes the surface is perfectly uniform. In reality, this fixed value does not account for small-scale fluctuations caused by different pile densities, types of infill (e.g., rubber or sand) and the physical wear and tear of the turf. Nevertheless, the

independent NDVI analysis (Table 9) provides strong empirical support for this clear separation, showing a stable contrast between AT (~0.05–0.21) and NG (~0.17–0.49) across all six acquisition dates.

Table 9. Median NDVI for all pitches.

		1 May	10 June	20 July	13 August	6 September	8 October
Koper	AT	0.203	0.193	0.202	0.192	0.213	0.208
	NG	0.436	0.301	0.413	0.392	0.404	0.390
Umag	AT	0.122	0.150	0.134	0.113	0.168	0.144
	NG	0.415	0.337	0.336	0.311	0.231	0.400
Novigrad	AT	0.129	0.140	0.116	0.115	0.147	0.126
	NG	0.443	0.391	0.401	0.370	0.400	0.379
Porec	AT	0.200	0.189	0.183	0.185	0.193	0.214
	NG	0.490	0.465	0.383	0.430	0.345	0.471
Rovinj	AT	0.117	0.115	0.105	0.101	0.127	0.107
	NG	0.435	0.370	0.392	0.401	0.321	0.390
Pula	AT	0.100	0.103	0.105	0.103	0.098	0.050
	NG	0.398	0.169	0.377	0.318	0.349	0.367
Medulin	AT	0.123	0.103	0.117	0.118	0.108	0.095
	NG	0.369	0.349	0.389	0.407	0.446	0.413

Furthermore, the timing of the Landsat overpass, at approximately 11:50 a.m., captures surfaces under high solar radiation but does so roughly 2–3 h before the daily thermal peak. Because synthetic materials lack the natural cooling mechanisms of vegetation, the thermal gap likely widens into the afternoon. Consequently, the results likely underestimate the true maximum difference in temperature during the hottest part of the day.

Finally, although pairs were selected for their proximity to ensure similar macroclimatic drivers, micro-scale variations remain unmeasured. In addition, factors such as the age of the AT, the specific type of rubber infill and the health of the NG were not taken into account. A critical unaccounted factor in this study is the specific maintenance of each site—specifically, active irrigation. In warmer climates, NG pitches are typically irrigated during summer months to maintain playability [14], allowing for cooling via evapotranspiration. Synthetic surfaces lack this internal regulation; even when occasionally watered, the rapid evaporation from synthetic fibres means they quickly return to a 'dry' state of high heat sensitivity. While the lack of a standardised watering schedule across the seven sites may have introduced thermal noise into the analysis, the per-date NDVI data provides direct evidence on this issue: median NDVI values for natural grass remained consistently high throughout the peak summer months of July and August across all locations (NDVI = 0.311–0.430). This confirms that the NG pitches were probably actively irrigated and maintained in a living, transpiring state during peak heat rather than undergoing seasonal senescence or dormancy. Although localized, late-summer vegetation stress was observed at isolated locations (e.g., Pula NG dropping to 0.169 in June, and Umag NG falling to 0.231 in September); the overall trajectory demonstrates that the thermal differences observed in this study primarily reflect a comparison between artificial turf and fully functional, irrigated natural grass, rather than unmanaged or dry vegetation.

3.7. Future Research

Future research should focus on using high-resolution thermal imaging to eliminate edge effects and provide more precise surface data. Specifically, higher-spatial-resolution sensors are required to overcome the mixed-pixel constraints of the current dataset and test

the hypothesis that thermal offsets extend to smaller-scale or non-standardized plasticised environments, such as parks, private gardens, and coastal developments.

It is also essential to track thermal trajectories throughout the entire day to capture the daily heat peak, which typically occurs several hours after satellite overpasses. Beyond sports pitches, there is a critical need to investigate other synthetic environments, such as rubber-based (tartan) playgrounds, to determine whether the widespread 'plasticisation' of recreational zones creates a systemic risk to public well-being. Such studies should address the fundamental paradox of infrastructure designed for health and recreation that may instead function as a hazardous thermal stressor.

Another possible research goal could be to compare AT with both irrigated and non-irrigated NG. This would help distinguish between the cooling effects of active watering and the inherent 'material advantage' of NG. Furthermore, comparing mown NG pitches to overgrown ones could address how effective mown NG is as a thermal solution for public spaces such as parks and beaches. This research is essential for shifting urban planning towards resilient green infrastructure that offers genuine heat mitigation compared to plasticised or high-maintenance landscapes.

4. Conclusions

The adoption of AT in the northern Adriatic region represents a fundamental shift in urban microclimates, moving from surfaces that naturally regulate heat to those that actively amplify it. While synthetic turf is often marketed as a durable and water-saving alternative to NG, these benefits are offset by a consistent and significant thermal penalty. Even under identical climatic conditions, synthetic surfaces maintained a significantly higher thermal regime: uncorrected LST revealed a median heat penalty of 3.84 °C (with peak differences up to 6.50 °C), while emissivity-corrected LST (cLST) expanded the thermal gap to a difference of 6.28 °C, with peak differences reaching up to 9 °C. This suggests that by replacing grass with synthetic polymers, cities are effectively installing permanent hot spots in an already warming region.

The difference between AT and NG was lower than those reported in previous studies [9,13–16]. While other studies often mentioned peak midday extremes of 30–60 °C, the current study's median heat penalty of 3.84–6.28 °C reflects an average across a broader range of times and weather conditions rather than just worst-case scenarios.

Rather than acting as a thermal buffer, AT operates at an elevated thermal baseline that closely tracks rising air temperatures ($\beta_{AT} = 1.110$). While pooled regression analysis indicates that the rate of thermal response to ambient warming does not differ significantly between surface types ($p = 0.6437$), AT consistently sustains a parallel, elevated surface heat profile across all observed temperatures.

This thermal impact is driven by the intrinsic heat-absorbing properties of synthetic polymers alongside surrounding urban built density. While surrounding impervious cover contributes approximately 0.67 °C of additional warmth for every 10% increase in background built density, the lack of a significant interaction between surface type and buffer imperviousness confirms that the thermal offset is primarily a characteristic of the surface material itself rather than a result of its surroundings. Under covariate control, AT retains a direct material thermal elevation of 4.99 °C over NG.

While sports pitches were the primary focus of the study because of their standardised dimensions, reliable satellite detection and maximum solar exposure, they serve as a representative model to highlight the broader hazards of the plasticisation of urban landscapes. The microclimatic impacts of replacing natural vegetation with synthetic polymers warrant further investigation across other built environments.

Ultimately, these findings point towards a critical need for a more nuanced approach to urban sports infrastructure. The convenience of lower maintenance and reduced water usage comes at a high environmental cost that is often overlooked in the planning phase. High NDVI values across the study sites confirmed that the thermal performance of NG pitches relied heavily on active irrigation, emphasizing that the microclimatic cooling benefits of natural turf are intrinsically tied to water management. If cities continue to prioritise synthetic surfaces, they must account for the resulting thermal degradation of the surrounding landscape. Crucially, spatial planning instruments must address current accounting contradictions—such as Koper's spatial plan classifying artificial turf as "green space"—by reclassifying synthetic pitches as artificial infrastructure and adjusting site-level planning metrics to reflect their inability to deliver fundamental ecological functions.

Future developments should reconsider the preservation of NG or other climate-adapted natural vegetation as a vital tool for microclimate regulation or, at the very least, explore cooling technologies for synthetic pitches that can better mimic the natural cooling of vegetation. Without such interventions, the expansion of AT will continue to undermine the thermal resilience of coastal cities.

Supplementary Materials: The following supporting information can be downloaded at https://www.mdpi.com/article/10.3390/land15112207/s1, Figure S1: Residual diagnostic plots for the linear mixed-effects model of the AT–NG temperature difference; Figure S2: Normal Q–Q plots of site and date random intercepts; Table S1: Data acquisition; Table S2: Full Land Surface Temperature (LST) zonal statistics; Table S3: Full Land Surface Temperature (LST) zonal statistics with corrected emissivity; Table S4: Retrieval uncertainty.

Author Contributions: Conceptualisation: F.V. and T.P.; methodology: F.V. and T.P.; software: F.V.; validation: F.V. and T.B.; formal analysis: F.V. and T.B.; investigation: F.V.; resources: F.V.; data curation: F.V.; writing—original draft preparation: F.V.; writing—review and editing: F.V., T.P. and T.B.; visualisation: F.V.; supervision: T.P.; project administration: T.P.; funding acquisition: T.P. All authors have read and agreed to the published version of the manuscript.

Funding: This research was funded by the Slovenian Research and Innovation Agency (ARIS) under research core funding no. P4-0009 (Landscape as a Living Environment) and by the Interreg VI-A Slovenia–Croatia project ZeleNatura: Improving Urban Infrastructure for Greener Cores of the Northern Adriatic (SIHR00182), which is co-funded by the European Union through the European Regional Development Fund.

Data Availability Statement: Landsat 8 and Landsat 9 Collection 2 Level-2 Surface Temperature products are publicly available from the U.S. Geological Survey (USGS) Earth Explorer repository (https://earthexplorer.usgs.gov/). Ground meteorological station data were retrieved from the Slovenian Environment Agency (ARSO) and the Croatian Meteorological and Hydrological Service (DHMZ). Detailed scene metadata, acquisition timestamps, and cloud cover percentages are itemized in Supplementary Table S1. The fourteen target pitch boundary shapefiles and the complete per-date zonal-statistics dataset are available in the Supplementary Material.

Conflicts of Interest: The authors declare no conflicts of interest. The funders had no role in the design of the study; the collection, analysis or interpretation of the data; the writing of the manuscript; or the decision to publish the results.

Notes

[1] To verify that pitch size variations across municipal pairs did not bias thermal observations, the relationship between the AT:NG area ratio and ΔLST was tested. Neither Pearson correlation ($r = 0.297$, $p = 0.057$) nor linear regression ($\beta = 3.989$, $p = 0.057$, 95% CI [−0.116, 8.095]) revealed a statistically significant relationship at the $\alpha = 0.05$ level.

[2] The six selected acquisition dates, corresponding WRS-2 tile identifiers, full Landsat Product IDs, scene identifiers, exact UTC acquisition timestamps, and per-scene cloud cover percentages are summarized in Supplementary Table S1.

[3] Estimated according to WMO-No. 8/CIMO guidelines based on site land cover and proximity to artificial surfaces.

References

1. Golden, L.M. The Contribution of Artificial Turf to Global Warming. *Sustain. Clim. Change* **2021**, *14*, 436–449. [CrossRef]
2. Cheng, H.; Hu, Y.; Reinhard, M. Environmental and Health Impacts of Artificial Turf: A Review. *Environ. Sci. Technol.* **2014**, *48*, 2114–2129. [CrossRef] [PubMed]
3. Yaghoobian, N.; Kleissl, J.; Krayenhoff, E.S. Modeling the Thermal Effects of Artificial Turf on the Urban Environment. *J. Appl. Meteorol. Climatol.* **2010**, *49*, 332–345. [CrossRef]
4. Francis, R.A. Artificial Lawns: Environmental and Societal Considerations of an Ecological Simulacrum. *Urban For. Urban Green.* **2018**, *30*, 152–156. [CrossRef]
5. Simpson, T.J.; Francis, R.A. Artificial Lawns Exhibit Increased Runoff and Decreased Water Retention Compared to Living Lawns Following Controlled Rainfall Experiments. *Urban For. Urban Green.* **2021**, *63*, 127232. [CrossRef]
6. Cumberbatch, I.; Richardson, L.; Grant-Bier, E.; Kayali, M.; Mbithi, M.; Riviere, R.; Xia, E.; Spinks, H.; Mills, G.; Tuininga, A. Artificial Turf Versus Natural Grass: A Case Study of Environmental Effects, Health Risks, Safety, and Cost. *Sustainability* **2025**, *17*, 6292. [CrossRef]
7. Seletković, A.; Kičić, M.; Ančić, M.; Kolić, J.; Pernar, R. The Urban Heat Island Analysis for the City of Zagreb in the Period 2013–2022 Utilizing Landsat 8 Satellite Imagery. *Sustainability* **2023**, *15*, 3963. [CrossRef]
8. Kaplan, G.; Avdan, U.; Avdan, Z.Y. Urban Heat Island Analysis Using the Landsat 8 Satellite Data: A Case Study in Skopje, Macedonia. *Proceedings* **2018**, *2*, 358. [CrossRef]
9. Williams, C.F.; Pulley, G.E. *Synthetic Surface Heat Studies*; West Coast Turf: Winchester, CA, USA, 2002. Available online: https://www.westcoastturf.com/getdoc.cfm?id=38&srsltid=AfBOopPfqqIJS5dADP46M9BJ5xVpomShW46DbDT4GQpnHH8jQKqvLT8 (accessed on 15 February 2026).
10. Devitt, D.; Young, M.; Baghzouz, M.; Bird, B. Surface Temperature, Heat Loading and Spectral Reflectance of Artificial Turfgrass. *J. Turfgrass Sports Surf. Sci.* **2007**, *83*, 68–82.
11. Ćesić, M.; Rogulj, K.; Krtalić, A. Combined Thermal Index Development for Urban Heat Island Detection in Area of Split, Croatia. *Land* **2025**, *14*, 175. [CrossRef]
12. Thoms, A.W.; Brosnan, J.T.; Zidek, J.M.; Sorochan, J.C. Models for Predicting Surface Temperatures on Synthetic Turf Playing Surfaces. *Procedia Eng.* **2014**, *72*, 895–900. [CrossRef]
13. Vyrlas, P.; Koutras, M.; Liakos, V. Surface Temperature Experienced and Irrigation Effects on Artificial Turf. *WSEAS Trans. Environ. Dev.* **2024**, *20*, 194–202. [CrossRef]
14. McNitt, A.S.; Petrunak, D.M.; Serensits, T.J. Temperature Amelioration of Synthetic Turf Surfaces through Irrigation. *Acta Hortic.* **2008**, *783*, 573–582. [CrossRef]
15. Jim, C.Y. Solar–Terrestrial Radiant-Energy Regimes and Temperature Anomalies of Natural and Artificial Turfs. *Appl. Energy* **2016**, *173*, 520–534. [CrossRef]
16. Singh, G.; Peterson, B.; Jay, O.; Stevens, C.J. The Effect of Synthetic Grass Sports Surfaces on the Thermal Environment: A Systematic Review. *Int. J. Biometeorol.* **2024**, *68*, 1235–1252. [CrossRef] [PubMed]
17. Mantas, V.M.; Xian, G. Land Surface Temperature Differences Between Natural and Artificial Turf Sports Fields as Estimated from Satellite: Examples from the United States and Europe. In Proceedings of the 2021 IEEE International Geoscience and Remote Sensing Symposium IGARSS, Brussels, Belgium, 11–16 July 2021; pp. 1777–1780. [CrossRef]
18. Cheung, P.K.; Livesley, S.J. The Microclimate, Surface Energy Flux and Human Skin Burn Risks of Artificial Turf as Compared to Natural Turf. *Build. Environ.* **2025**, *273*, 112679. [CrossRef]
19. Liu, Z.; Jim, C.Y. Playing on Natural or Artificial Turf Sports Field? Assessing Heat Stress of Children, Young Athletes, and Adults in Hong Kong. *Sustain. Cities Soc.* **2021**, *75*, 103271. [CrossRef]
20. de Haan, W.P.; Quintana, R.; Vilas, C.; Cózar, A.; Canals, M.; Uviedo, O.; Sanchez-Vidal, A. The Dark Side of Artificial Greening: Plastic Turfs as Widespread Pollutants of Aquatic Environments. *Environ. Pollut.* **2023**, *334*, 122094. [CrossRef] [PubMed]
21. Russo, C.; Cappelletti, G.M.; Nicoletti, G.M. The Product Environmental Footprint Approach to Compare the Environmental Performances of Artificial and Natural Turf. *Environ. Impact Assess. Rev.* **2022**, *95*, 106800. [CrossRef]
22. Mestna občina Koper. Občinski Prostorski Načrt Mestne Občine Koper. 2022. Available online: https://www.koper.si/wp-content/uploads/2022/02/11_odlok_cistopis.pdf (accessed on 27 September 2024).
23. Massini, G.; Recondo, C.; Peón, J. Biotope Area Factor: An Ecological Urban Index to Geovisualize Soil Sealing. *Sustainability* **2020**, *12*, 150. [CrossRef]
24. Stad, M. *Grönytefaktor för Kvartersmark [Green Space Factor for Built-Up Area]*; Environmental Department, City of Malmö: Malmö, Sweden, 2020.
25. Gustin, M.; Fleming, P.R.; Allinson, D.; Watson, S. Modelling Surface Temperatures on 3G Artificial Turf. *Proceedings* **2018**, *2*, 279. [CrossRef]
26. Schiavon, M.; Shiflett, S.; Baird, J.H.; Geis, L.A.; Scudiero, E. Southern California Land Surface Temperature Differences under Different Landscape Composition. *Agron. J.* **2024**, *116*, 2678–2689. [CrossRef]

27. Fang, R.; Shan, X.; Deng, Q. Research on Air Temperature Inversion Method Based on Land Surface Temperature of Different Land Surface Cover. *Atmosphere* **2025**, *16*, 754. [CrossRef]
28. Yang, Y.; Tang, S. Urban Stadiums as Multi-Scale Cool-Island Anchors: A Remote Sensing-Based Thermal Regulation Analysis in Shanghai. *Remote Sens.* **2025**, *17*, 2896. [CrossRef]
29. Zhou, D.; Zhao, S.; Zhang, L.; Sun, G.; Liu, Y. The Footprint of Urban Heat Island Effect in China. *Sci. Rep.* **2015**, *5*, 11160. [CrossRef] [PubMed]
30. Jim, C.Y. Intense Summer Heat Fluxes in Artificial Turf Harm People and Environment. *Landsc. Urban Plan.* **2017**, *157*, 561–576. [CrossRef]
31. Lateef, M.B.; Aderotoye, D. Robust Satellite Technique Detection of Extreme Heat Events in Italy: A 26-Year (2000–2025) Study of Non-Stationary Thermal Baselines. *Urban Build. Sci.* **2026**, *1*, 100024. [CrossRef]
32. Malakar, N.K.; Hulley, G.C.; Hook, S.J.; Laraby, K.; Cook, M.; Schott, J.R. An Operational Land Surface Temperature Product for Landsat Thermal Data Standard Collection 2. *Remote Sens. Environ.* **2018**, *204*, 148–162. [CrossRef]
33. NASA Land Processes Distributed Active Archive Center. *ASTER Global Emissivity Dataset (GED) V003 [Dataset]*; NASA Land Processes Distributed Active Archive Center: Sioux Falls, SD, USA, 2014.
34. Shi, Y.; Jim, C.Y. Developing a Thermal Suitability Index to Assess Artificial Turf Applications for Various Site-Weather and User-Activity Scenarios. *Landsc. Urban Plan.* **2022**, *217*, 104276. [CrossRef]
35. Voogt, J.; Oke, T. Thermal Remote Sensing of Urban Climates. *Remote Sens. Environ.* **2003**, *86*, 370–384. [CrossRef]
36. U.S. Geological Survey. *Landsat 8-9 Collect. 2 (C2) Level-2 Science Product (L2SP) Guide (Version 2.0)*; United States Geological Survey: Asheville, NC, USA, 2020.
37. Sobrino, J.A.; Jiménez-Muñoz, J.C.; Paolini, L. Land Surface Temperature Retrieval from LANDSAT TM 5. *Remote Sens. Environ.* **2004**, *90*, 434–440. [CrossRef]
38. Esposito, A.; Pappaccogli, G.; Buccolieri, R. Surface Urban Heat Island (SUHI) Dynamics in the Major Apulian Cities Using Remote Sensing Approaches. *Bull. Atmos. Sci. Technol.* **2026**, *7*, 22. [CrossRef]

Disclaimer/Publisher's Note: The statements, opinions and data contained in all publications are solely those of the individual author(s) and contributor(s) and not of MDPI and/or the editor(s). MDPI and/or the editor(s) disclaim responsibility for any injury to people or property resulting from any ideas, methods, instructions or products referred to in the content.